Current Research in Translational Medicine 73 (2025) 103532

Contents lists available at ScienceDirect

Current Research in Translational Medicine

journal homepage: www.elsevier.com/locate/retram

Original article

Effect of adipose-derived mesenchymal stromal/stem cells on mouse mammary tumour growth and formation of lung metastases

Kimberly T. Peta [a], Chrisna Durandt [a], Marlene B. van Heerden [b], Michael S. Pepper [a], Melvin A. Ambele [a,b,*]

[a] Institute for Cellular and Molecular Medicine, Department of Immunology, and SAMRC Extramural Unit for Stem Cell Research and Therapy, Faculty of Health Sciences, University of Pretoria, Gezina, Pretoria, 0084, South Africa
[b] Department of Oral and Maxillofacial Pathology, School of Dentistry, Faculty of Health Sciences, University of Pretoria, PO Box 1266, Pretoria 0001, South Africa

ARTICLE INFO

Keywords:
Mesenchymal stromal/stem cells
Breast cancer
Tumour growth
Tumour progression
Tumour metastasis

ABSTRACT

Background: The role of mesenchymal stromal/stem cells (MSCs) in tumour development and progression remains a subject of debate. Previous studies have reported contradictory outcomes, possibly due to variations in experimental design and the use of xenograft models. Xenograft models limit interpretation and translation due to cross-species variability. To address these limitations, we employed an isogenic mouse model of spontaneous breast cancer (BC) to investigate the impact of murine MSCs on BC development and progression. Methods: MSCs isolated from FVB/N mouse adipose tissue (mASCs) were administered to female mice with palpable mammary tumours. Tumour volume and mass were assessed, and analysis of histopathological necrosis and gene expression was conducted on mammary (MT) and lung metastatic tumours (LT). Results: No change in MT mass and volume was observed between mASC-treated and control mice. However, mASC treatment led to increased necrosis in LT but not in MT. Immunohistochemistry revealed that mASC-treated mice had fewer CD163+ anti-inflammatory macrophages in the LT but not in the MT. Tgf-β3, vegfr1, and cd105 were observed and downregulated in both MT and LT in mASC-treated mice. The downregulation of cd36 and tgf-β3 contributes to pro-tumourigenic activities, whereas the downregulation of vegfr1 and cd105 is associated with an anti-tumour effect. In the mASC treatment group, all cytokines tested for, except IL-27, were elevated. Conclusion: This study suggests that mASCs are anti-tumourigenic in pulmonary metastatic BC. Our findings emphasize the importance of considering the tumour microenvironment and employing relevant animal models when investigating the impact of MSCs on tumour progression.

1. Introduction

Breast cancer (BC) is the most prevalent cancer in females and the leading cause of cancer death [1,2]. In 2020, 2.3 million new female BC cases were diagnosed worldwide with over six hundred thousand deaths recorded. BC accounts for 1 in 6 cancer mortalities and 1 in every 4 cancer cases in women [2]. Current BC treatments, including mastectomy, tumourectomy, chemotherapy, hormone therapy, and radiotherapy have improved the 5-year survival rate. However, these treatments lack specificity as they indiscriminately target both cancerous and healthy cells and are often ineffective against advanced and metastatic BC [3,4]. To address these challenges, there is a need for treatments that selectively target cancer cells. One potential approach is the use of mesenchymal stromal/stem cells (MSCs), a heterogeneous population of cells that morphologically resemble fibroblastic cells [5–7]. MSCs can be isolated from most adult tissues, with adipose tissue (ASCs), bone marrow (BM-MSCs), and umbilical cord (UC-MSCs) being the most frequently used [5]. Multipotent MSCs have the capacity to self-renew and are able to differentiate into adipocytes, osteoblasts, chondrocytes, and other cell types [5,6]. MSCs possess regenerative and immunomodulatory properties, making them an attractive candidate for cellular and immuno-therapy [8]. MSCs are reported to “home” to the tumour microenvironment (TME) where they elicit an immune response that either promotes (pro-tumorigenic) or suppresses tumour

Institute for Cellular and Molecular Medicine, Department of Immunology; and SAMRC Extramural Unit for Stem Cell Research and Therapy, Faculty of Health Sciences, University of Pretoria, Gezina, Pretoria, 0084, South Africa.
* Corresponding author.
E-mail address: melvin.ambele@up.ac.za (M.A. Ambele).

https://doi.org/10.1016/j.retram.2025.103532
Received 10 January 2024; Accepted 27 July 2025
Available online 28 July 2025

(anti-tumorigenic) progression [9].

Adipose tissue is rich in MSCs, containing 500-fold more of these cells per gram of tissue than MSCs present in a similar volume of bone marrow [10]. Breast tissue is mainly composed of adipose tissue (fat cells) and serves as an important endocrine organ by secreting signalling molecules that regulate various cellular processes [10]. The secretory profiles of breast adipocytes of BC patients and healthy controls differ, and it has been suggested that growth factors and other signalling molecules secreted by breast adipose tissue contribute to BC development and progression [11].

Numerous studies, both in vitro and in vivo, have investigated the role of MSCs on BC progression [12–15]. Several studies indicated that ASCs promote BC cell proliferation, migration, and invasion [16–19]. Moreover, in vivo experiments have demonstrated that ASCs induce primary tumour growth, epithelial-to-mesenchymal transition (EMT), angiogenesis, and metastasis [8,20–23]. ASCs secrete several cytokines such as IL-6, IL-8, VEGF, IL-10, TGFβ−1, MMPs, chemokine ligand 2 (CCL2) and CCL5 resulting in elevated levels in the TME, which is suggested to stimulate BC progression [18,24–28]. Additionally, metastatic lesions are often observed in the lungs and occasionally in the liver and spleen of BC patients [8,21,22]. Interestingly, reducing the expression of leptin, a hormone associated with obesity, in obesity-altered ASCs (obASCs) in SCID mice, resulted in decreased primary tumour volume and a significant reduction in the number of metastatic lesions in the liver and lung [29,30]. Furthermore, it has been suggested that mutations in BC-associated genes such as BRCA1, present in ASCs, can promote the invasion and growth of BC [27]. Notably, mouse adipose mesenchymal stromal/stem cells (mASCs) have been observed to promote tumour growth and metastasis through increased secretion of insulin-like growth factor-1 [8,20]. These findings underscore the significant impact of ASCs on BC progression and highlight the complex interplay between these cells and TME.

In contrast, a considerable body of evidence suggests that ASCs exert an inhibitory effect on BC progression [31–39]. These studies have shown that ASCs significantly decrease BC cell proliferation, promote BC cell apoptosis, reduce BC cell invasion and tumour migration, reduce tumour mass, and slow tumour growth rate [34,35,40]. In vitro experiments conducted by Clark et al. (2015) using immortalized BC cell lines (MDA-MB-231 and T47D) demonstrated that ASCs inhibit BC cell migration and invasion through the secretion of tissue inhibitors of metalloproteinase inhibitors, TIMP-1 and TIMP-2 [39]. Moreover, ASCs have been found to inhibit BC by downregulating EMT genes such as TWIST1, CDH2, Snail1, and Snail2 [37]. The production of exosomes by ASCs has been associated with decreased BC cell viability [40]. In summary, there is currently no consensus regarding the effect of ASCs on BC progression, and more studies are needed to understand the interactions between ASCs and BC cells [27].

The contradicting findings of the effect of ASCs on BC tumour progression have been extensively reviewed by (Oloyo et al. (2017)) [41], who concluded that the significant variation in experimental design/approaches is one of the major contributors to the different outcomes observed. Study approaches range from using either primary human-derived ASCs isolated from mammary tissue or lipo-aspirates, human-derived ASCs isolated from breast tissue from mastectomies of BC patients [17,22,27,36,38], or mouse-derived primary ASCs [42–44] to investigate the effect of ASCs on human-derived immortalized BC cell lines, such as MCF-7, MDA-MB-231, ZR-75–1, T47D, BT-474, CG5, SK-BR-3, HCC1937 and MDA-MB-435 [18,19,22,23,31,36] or murine breast carcinoma cells such as E0771, 4T1 and Met-1 [8,20].

Both xenograft and allograft experimental models have been used to investigate the effect of ASCs on the development, progression, and metastasis of BC. Allograft experimental models have investigated the effect of mASCs on mouse mammary adenocarcinoma cells [20,34,35], while xenograft experimental models utilized human BC cells and human ASCs in experimental animal models [18,19,22,23,31,36]. Moraes et al. (2016) and Li et al. (2020) used an allograft experimental design whereby BALB/c and C57BL/6 J mice developed tumours after receiving 4T1 and E0771 BCE cell lines injected into their fat pads. A week later, these animals received mouse ASCs (mASCs) derived from gonadal adipose tissue and inguinal fat pads from C57BL/6 J mice. The mice received ASCs with either CD90high or CD90low extracellular vesicles (EVs). In comparison to ASCs-CD90high, ASCs-CD90low resulted in significantly reduced tumour mass and slower tumour growth rate [34,35]. These studies demonstrated that ASCs, whether directly or indirectly inhibit the progression of BC.

The aim of this study is to address the conflicting findings on the impact of ASCs on BC progression. To achieve more physiologically relevant observations and enhance translational potential in the human setting, we propose a novel approach in investigating the impact of mASCs on BC progression and metastasis using an isogenic mouse model of spontaneous mammary tumour development. This approach more accurately recapitulates what might occur in patients who incidentally have a small or latent tumour, and who might receive autologous ASCs for a variety of therapeutic purposes, unrelated to tumorigenesis per se, for example for regenerative medicine indications. Our hypothesis posits that mASCs will exert an impact on tumours.

We conducted a study to investigate the effect of mASC treatment on BC progression and metastasis using an isogeneic FVB/N-Tg(MMTV-PyVT)634Mul/J mouse model. These mice contain the MMTV-PyVT (mouse mammary tumour virus- polyoma virus middle T antigen) transgene, which induces the spontaneous development of primary mammary tumours [45]. We examined genes involved in tumour invasion, angiogenesis, and metastasis such as cd36, endoglin (cd105), transforming growth factor-beta 3 (tgf-β3), vascular endothelial growth factor receptor 1 (vegfr1) and metadherin (mtdh) [46–51]. Additionally, we performed immunohistochemical analysis to assess the presence of CD3 and M2-associated (CD163-positive) macrophages. Our findings provide important contributions to the understanding of ASC-based treatments for BC.

2. Materials and methods

2.1. Animal studies

The study was approved by the Faculty of Health Sciences Research Ethics Committee (ethics reference no.: REC166–19) and the Animal Ethics Committee (ethics reference no.: 534/2019) of the University of Pretoria. Animal husbandry was conducted at the Onderstepoort Veterinary Animal Research Unit (OVARU). FVB-TgN(MMTV-PyVT) mice were purchased from Jackson Laboratory (Jackson Laboratory; Bar Harbor, ME, USA) and were used for breeding and isolation of mASCs. To obtain heterozygous offspring, hemizygous males were bred with wild-type females. The resulting offspring were genotyped, and the heterozygous females were recruited into the study while the heterozygous males were used for breeding. A total of 20 heterozygous female mice ($n = 10$ for mASC-treatment group and $n = 10$ for the control group) were used for this study.

2.2. Genotyping

The KAPA Mouse Genotyping Kit (KAPABIOSYSTEM, Cape Town, South Africa) was used for genotyping according to the manufacturer's instructions. Briefly, DNA was extracted from 2 mm mouse tail biopsies and placed in 0.2 mL microcentrifuge tubes. The forward primer 5-' CAAATGTTGCTTGTCTGGTG-3′ and reverse primer 5′-GTCAGTC-GAGTGCACAGTTT-3′ specific for internal positive control and the forward primer 5′- GGAAGCAAGTACTTCACAAGGG-3′ and reverse primer 5′- GGAAAGTCACTAGGAGC GGG-3′ specific for the transgene was used in the PCR genotyping experiment. The two pairs of primer sequences were obtained from the Jackson Laboratory website (Jackson Laboratory; Bar Harbor, ME, USA). Amplification was done using a thermocycler (GeneAmp® PCR System 9700) for 35 cycles under the following

conditions: Initial denaturation at 95 °C for 3 min, denaturation at 95 °C for 15 s, annealing at 60 °C for 15 s, and extension for 15 s for 2 min. The amplicons were stained with ethidium bromide and separated on a 2 % agarose gel electrophoresis to determine the size.

2.3. mASC isolation and in vitro expansion

The inguinal white adipose tissue (ingWAT) excised from wild-type FVB/N mice under sterile conditions, was placed in a tissue culture dish and minced in a biosafety cabinet (ESCO, BSC class II). The minced tissue was transferred into 30 mL digestion medium (pre-prepared) that constituted of 0.8mg/mL collagenase II (Gibco, ThermoFisher, MA, USA,) dissolved in tissue medium ((1 % fatty acid-free bovine serum albumin (BSA) (Sigma-Aldrich, Darmstadt, Germany)) dissolved in Hanks' balance salt solution (Sigma-Aldrich, Darmstadt, Germany), and placed in a water bath at 37 °C for 45 min (vortexed every 5minutes). The digested tissue was then filtered through a 200 μm nylon mesh into a 50 mL tube containing 10 mL complete culture media (CCM; 20 % foetal bovine solution (FBS) (Gibco, ThermoFisher, MA, USA), 2 % Pen/Strep (Gibco, ThermoFisher, MA, USA), 1 % glutamine (Sigma-Aldrich, Steinheim, Germany) and 0.2 % amphotericin (Sigma-Aldrich, Steinheim, Germany) in DMEM/F-12 (Lonza, Whitesci, Switzerland)]. The filtrate was centrifuged (SL-16R, Thermo Scientific) at 500 g for 7 min after which the supernatant was aspirated leaving behind the pellet. The mASC pellet was resuspended in CCM, plated at 5×10^3cells/cm³ in 75 cm³ culture flasks and placed in a 37 °C/5 % carbon dioxide (CO2) incubator (Labotec, Thermo Scientific). The cell culture medium was changed twice a week and cells were passaged when they became confluent. At passage 5, mASCs were cryopreserved by resuspending dissociated cells in freezing medium (70 % FBS, 20 % Dulbecco's modified eagle medium/F12 (DMEM/F12) supplemented with 10 % dimethyl sulfoxide (DMSO)), transferred to cryovials (Lasec, Greiner Darmstadt, Germany) and stored in liquid nitrogen vapour (Statebourne biorack 4800, Thermo Scientific, Washington, UK). To thaw the mASCs, 700 μL of FBS was added to the cryovials and centrifuged at 500 g for 7 min and then plated at 5×10^3cells/cm³ in 75 cm³ culture flasks. The mASCs used for this study were at passages 6 to 8.

2.4. Characterization of mASCs

The immunophenotypic profile and adipogenic and osteogenic differentiation capabilities of the mASCs were determined before the cells were used in vivo experiments.

2.4.1. Flow cytometric analysis of mASCs

mASCs were immunophenotyped at passage 3 using a Cytoflex flow cytometer (Beckman Coulter, Florida, USA). Immunophenotyping was done as previously described with some modifications [52]. Briefly, mASCs were washed twice using PBS and dissociated by adding 7 mL trypsin (GIBCO, Life Technologies™, New York, USA), followed by incubation for 4 min in a 37 °C/5 % CO2 incubator. An equal volume of CCM was added to the dissociated cell suspension followed by centrifugation at 500 g for 7 min. An aliquot of the cell suspension (100 μL) was transferred to a flow cytometry tube, after which 5 μL of each antibody was added to the cells and incubated for 15 min in the dark. The anti-mouse antibodies used to stain the cells were CD45-Brilliant Vio-let 421 (30-F11) (Biocom, Biolegend, San Diego, CA, USA), CD90.2-APC (53–2.1), CD31-PE (390), CD29-FITC (HMb1–1), CD105-PE-C7 (MJ7/18) and CD106-PE-C7 (429) purchased from eBioscience, Invitrogen (San Diego, CA, USA). The cells stained with CD105 were processed in a separate tube because this marker has the same fluoro-chrome as CD106. The data was analysed using Kaluza Flow Cytometry analysis software 1.2 (Beckman Coulter, Miami, USA).

2.4.2. Adipogenic and osteogenic differentiation

For adipogenic differentiation, mASCs were plated at a density of 2000 cells/cm³ in a 6-well plate. The cells were differentiated into the adipogenic lineage as previously described [52] with slight modifications. Briefly, CCM was added to cells at passage 3 to serve as non-induced controls (3 wells); adipogenic induction cocktail consisting of Dulbecco's Modified Eagle's Medium (GIBCO, Life Technologies™, New York, USA) supplemented with 20 % FBS, 2 % Pen/Strep, 10 μg/mL insulin (Gibco, ThermoFisher, MA, USA), 0.5 mM 3-isobutyl-methylxanthine (IBMX), 5 mM dexamethasone, 200 μM indomethacin. Indomethacin, IBMX, and dexamethasone were purchased from Sig-ma-Aldrich, Darmstadt, Germany. After a differentiation period of 21 days, cells were stained using 2.5 μg/mL 4′, 6-diamino-2-phenylindole, dihydrochloride (DAPI) (Life Technologies, Oregon, USA) and 50 ng/mL Nile red (Life Technologies, Oregon, USA). Images were captured at 10X magnification using a ZEISS Axio Vert.A1 inverted microscope (Carl Zeiss, Gottingen, Germany). For osteogenic differentiation, 2000 cells/cm³ were plated in a 6-well plate at passage 3. The differentiation procedures were performed as described by Seavey et al. [53], with the exception that cells were differentiated for 21 days instead of 14 days as described by the authors. Osteoblast staining was performed as described by Koch et al., 2007 [54], with a few minor modifications. In summary, the culture media was removed, and 10 % formalin was added to the cells followed by incubation for 1 hour at room temperature RT. After fixation, the cells were stained with 2 % alizarin red for 45 min at RT. The solution was aspirated, the wells were washed 4 times with dH2O, and 1 mL PBS was added.

2.5. mASC-treatment and tumour measurements

Experiments done on both control (untreated) and treatment groups were performed on 10 mice each. Each mouse in the mASCs treatment group received 2×10^6 mASCs suspended in 100 μL 0.9 % SABAX saline solution (Adcock Ingram, South Africa) through intraperitoneal injection (IP) on days 30 and 37 (from the time of birth). On day 44, the mice received 1.6×10^6 mASCs; the adjustment was due to the number of mASCs available and was made to ensure that all animals received the same number of cells. Each mouse in the treatment group thus received a total number of 5.6×10^6 mASCs over a period of 44 days. Mice in the control group received 100 μL of saline solution at each time point; the administration route was the same. Palpable primary tumours were measured once a week until termination, using a calliper to determine tumour volume. Volume was calculated using the formula L x W^2 / 2; L (length) and W (width). At termination, the mammary tumours were excised and weighed (Sartorius, Göttin-gen, Germany) to determine the tumour mass [in grams (g)] per animal.

2.6. Histology and immunohistochemistry

Mammary and lung tissues were collected from mice in both (control and mASC-treated) groups after they were euthanized and fixed in 10 % neutral buffered formalin (NBF). Haematoxylin and eosin staining was performed as previously described by Dhanraj et al.,2021 and Pitere et al., 2022 [55,56]. To visualize CD163-positive macrophages, the tissues were processed and stained, with minor modifications, using a rabbit monoclonal anti-mouse antibody directed against CD163, as previously described [55,56]. Briefly, 3-micron sections were cut from formalin-fixed paraffin-embedded (FFPE) tissue blocks and baked overnight in a 58 °C oven. Slides were deparaffinized in xylene, hydrated with decreasing concentrations of alcohol, and washed with distilled water. Endogenous peroxidase was quenched in 3 % hydrogen peroxide for 5 min at 37 °C. Antigen retrieval was performed in high pH buffer (Dako Envision FLEX Retrieval solution high pH, Agilent Technologies, Denmark), after which the sections were rinsed in phosphate-buffered saline (PBS) followed by blocking the background staining with protein block (NovolinkTM Leica Biosystems, Newcastle Upon Tyne, UK) for 30 min at room temperature to reduce background staining. Sections were incubated overnight at 4 °C in a 1:300 rabbit

monoclonal anti-CD163 antibody [EPR19518] (ab182422) (Abcam, Cambridge, UK). Slides were once again rinsed in PBS and detection was performed using an anti-rabbit NovolinkTM Polymer Detection Kit (Leica Biosys-tems) for 25 min at RT. Slides were once again washed in PBS and chromogen detection was performed (4 min at 37 °C) using 3, 3′-Diaminobenzidine (DAB) (NovolinkTM Polymer Kit). Sections were rinsed and counterstained in haematoxylin for 1 min. Dehydration in alcohol, clearing in xylene, and mounting in DPX followed. Negative controls were performed by substituting the anti-CD163 antibody with PBS. For CD3 IHC, 3-micron sections were cut, and the process was performed similarly to CD163 with a few differences. Antigen retrieval was performed in a low pH buffer (Cell Condition-ing Solution CC2, Ventana Medical Systems, Inc Arizona USA). Sections were incubated with a 1:100 rabbit monoclonal anti-CD3 (Abcam ab16669, clone SP7) antibody at room temperature for 120 min. Slides were rinsed in PBS and detection was performed using anti-rabbit Polymer HRP IgG (NovolinkTM Polymer Detection Kit, Leica Biosystems) for 30 min at RT. Negative controls were performed substituting the CD3 antibody with PBS. Images were captured at 40X magnification using a Leica AT 2 Aperio scanner (Leica Biosystems, Nussloch, Germany) and analyzed using Qupath software, version 0.2.3 (The Queens University of Belfast, Northern Ireland).

2.7. mRNA isolation and RT-qPCR

Total cellular mRNA was extracted from mammary and lung tissues of treated and untreated mice using the E.Z.N.A.® Total RNA Kit I (Omega Bio-Tek, Norcross, GA) following the manufacturer's instructions. The quality of mRNA was determined using the Nanodrop spectrophotometer (Inqaba Biotec, South Africa). Complementary DNA (cDNA) was generated from mRNA using the SensiFAST™ cDNA synthesis kit (Meridian Bioscience®, USA) according to the manufacturer's instructions and was quantified using a Nanodrop spectrophotometer. TaqMan RT-qPCR was used to determine the expression of the following genes: cd105 (Mm00468252_m1), tgf-β3 (Mm00436960_m1), vegfr1 (Mm00438980_m1), mtdh (Mm00482588_m1) and cd36 (Mm00432403_m1). The reference gene used was gapdh (Mm99999915_g1). For RT-qPCR, a 15 μL master mix containing 10 μL TaqMan fast advanced master mix (2X), 1 μL TaqMan assay probe (20X), 4 μL nuclease-free water and 5 μL (30 ng/μL) cDNA (sample template) were added to wells in a 96-well plate. The plate was run in standard mode on a QuantStudio™ 6 Flex Real-time PCR (Applied Biosystems™, MA, USA) under the following conditions for 40 cycles: incubation at 50 °C for 2 min, polymerase activation at 95 °C for 10 min, denaturation at 95 °C for 15 s, extension at 60 °C for 1 min. The software of QuantStudio 6 and 7 measured the threshold limit (Ct value) and the comparative CT method was used to calculate gene expression fold changes using the formula: ΔCT = CT average mASC – CT average reference gene, ΔCT = CT average control – CT average for reference genes; ΔΔCT= ΔCT mASCs - ΔCT control; Fold change = 2^{-}ΔΔCT.

2.8. Measurement of plasma cytokines

Approximately 800 μL of blood was collected in EDTA tubes through cardiac puncture and centrifuged at 14 000 rpm for 15 min. Approximately 250–300 μL of plasma was collected from each sample into 2 mL microcentrifuge tubes. The Legendplex mouse inflammation panel (13-plex) kit (Biolegend®, San Diego, CA, USA) was used for cytokine profiling. The assay was performed according to the manufacturer's instructions. The levels of the following 13 mouse cytokines were determined: Interleu-kin-23 (IL-23), IL-1α, interferon-gamma (IFN-γ), tumour necrosis factor-alpha (TNF-α), monocyte chemoattractant protein-1 (MCP-1), IL-12p70, IL-1β, IL-10, IL-6, IL-27, IL-17A, IFN-β, and granulocyte-macrophage colony-stimulating factor (GM-CSF). Cytokine levels (present in standards and samples) were measured using the Cytoflex flow cytometer (Beckman Coulter, California, USA). Standard curves were generated according to the manufacturer's instructions. Cytokine concentration levels were determined using the LEGENDplesTM data analysis software [version 8.0; BioLegend, San Diego, USA (https://legendplex.qognit.com/)]. All analysis was done using Biolegend's data analysis software.

2.9. Statistical analysis

Statistical analysis was performed using GraphPad Prism (version 5; GraphPad Software Inc., San Diego, CA, USA). Data was expressed as mean ± standard error of the mean (SEM). Two-tailed unpaired Student T-test was used to compare means between two groups. A two-way ANOVA and multiple comparison test were used to compare means of more than two categories.

3. Results

3.1. Characterization of mASCs: immunophenotype and differentiation potential

To confirm that the cells used were mASCs, they were immunophenotyped using a panel of anti-mouse antibodies. The mASCs were positive for CD29, CD105, and negative for CD31, CD106, CD45, and CD90.2. The majority of mASCs (99.58 %) did not express CD31 (an endothelial marker) but expressed CD29, of which 94.38 % lacked the expression of CD106 and CD45 (Fig 1A-B). Moreover, 98.79 % of these cells co-expressed CD29 and lacked CD90.2 (Fig 1C). The mASCs (99.85 %) also expressed CD105 (Fig 1D)), confirming their identity as mASCs.

To validate the multipotent differentiation potential, adipogenic and osteoblastic differentiation were assessed in mASCs. Adipogenic induction resulted in the accumulation of lipid droplets within the cells, confirming adipogenic differentiation. In contrast, non-induced cells showed the absence of lipid droplets (Fig 2A-B). Additionally, osteogenic differentiation was evident by the presence of calcium deposits, visually observed as red staining in the induced cells, whereas non-induced mASCs did not undergo differentiation (Fig 2C-D). These findings demonstrate that mASCs possess the capacity to differentiate into adipocytes and osteoblasts, confirming their multipotency.

3.2. mASC treatment initiates earlier tumour formation but does not impact tumour progression

To test for the effect of mASC treatment on tumour growth and progression, the size of mammary tumours was measured once a week for 4 weeks using a calliper. Measurements commenced after mice received the last dose of mASCs. Each mouse in the mASC group received 2×10^{6} cells on days 30, 37, and 1.6×10^{6} cells on day 44; therefore, the mASC-treated received a total of 5.6×10^{6} cells over a 14-day period. Notably, on week 3 after treatment, a larger number of mice (60 %) in the mASC treatment group exhibited palpable tumours earlier, compared with 30 % in the control group (Fig 3A). This observation suggests that the administration of mASCs resulted in earlier tumour initiation. At the point of termination, tumours were removed, measured (size), volume calculated, and weighed to determine tumour mass. No significant difference was observed in tumour volume ($p = 0.7782$) and mass ($p = 0.6411$) on average between the mASC-treated and untreated groups (Fig 3B-C). These findings indicate that while mASCs may have contributed to the initiation of tumour formation, they did not influence tumour progression.

3.3. Differential effects of mASC treatment on tumour necrosis: less necrosis in mammary tumours and higher levels of pulmonary necrosis

Histopathological analysis was performed on mammary tumour and lung tissue sections to evaluate the effects of mASC treatment. H&E staining was applied to five sections from each group (mASC-treated and

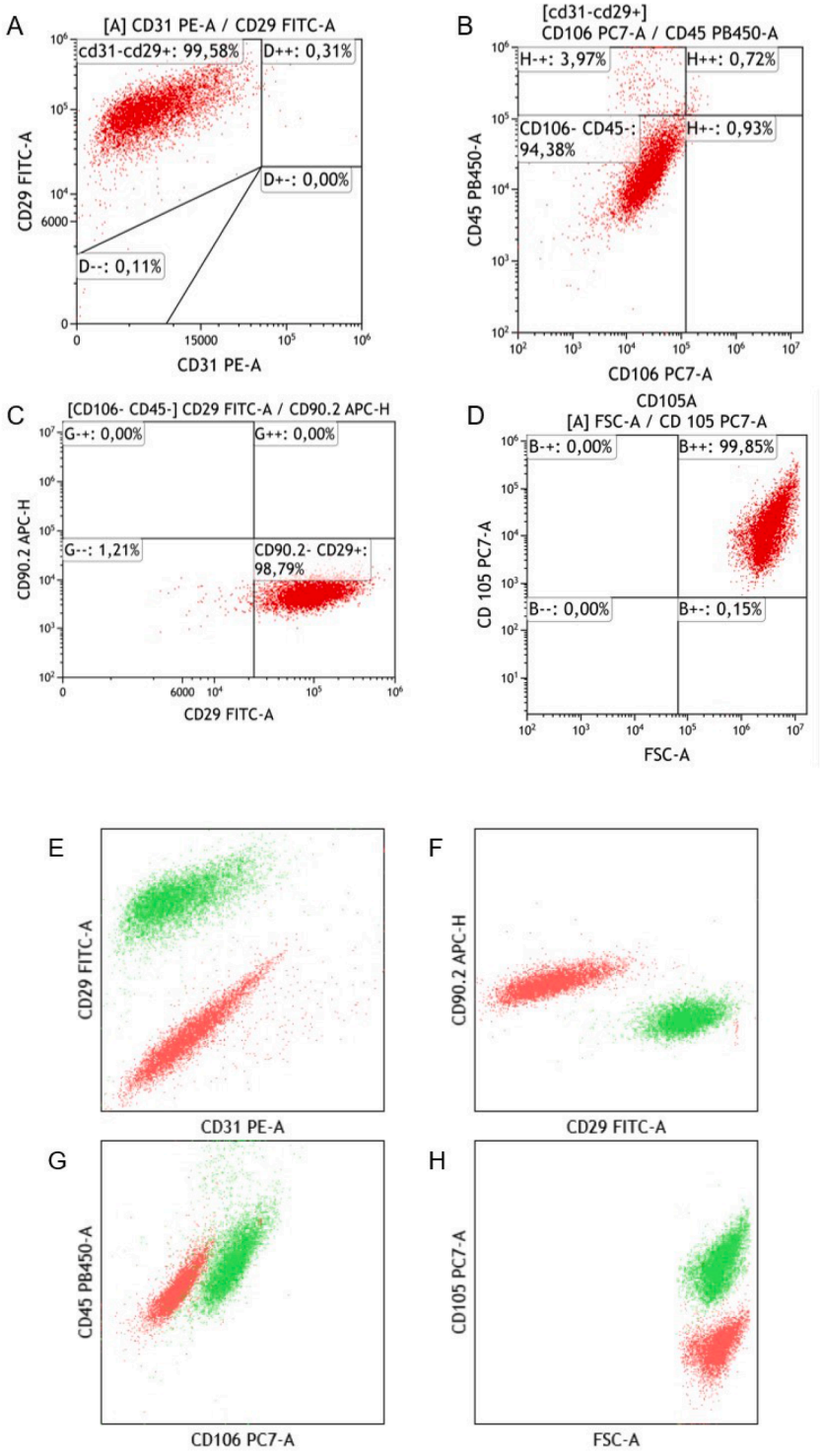

Fig 1. Representative flow cytometry two-parameter plots of mASC immunophenotype: (A-D) Two-parameter flow cytometry plots indicate that mASCs were positive for CD29 and CD105 and negative for CD31, CD45, CD90.2 and CD106. Plots A – H were gated (region A) on viable, intact ASCs. (E-H). Overlay dot plots indicate the isotypic controls (negative control) (green) and cells that were stained with the respective monoclonal antibodies (red).

control) to visualize tissue morphology. Manual delineation of boundaries was conducted to identify necrotic areas and calculate the degree of tumour necrosis. Red boundaries were drawn around the necrotic regions and a blue boundary encompassed the entire tissue section (Fig 4A-B). Tumour necrosis was measured by dividing the total sum of the necrotic areas by the area of the entire tissue section to determine the percentage of necrosis observed. mASC-treated mice exhibited less tumour necrosis ($p = 0.3486$) compared to the control group (Fig 4C). However, higher levels of pulmonary necrosis were observed in mASC-treated mice (Fig 4D). Although the result was not statistically significant, a p-value of 0.0882 suggests that mASC treatment promotes tumour cell necrosis. Our results suggest that mASC treatment inhibited necrosis in primary mammary tumours but enhanced pulmonary necrosis.

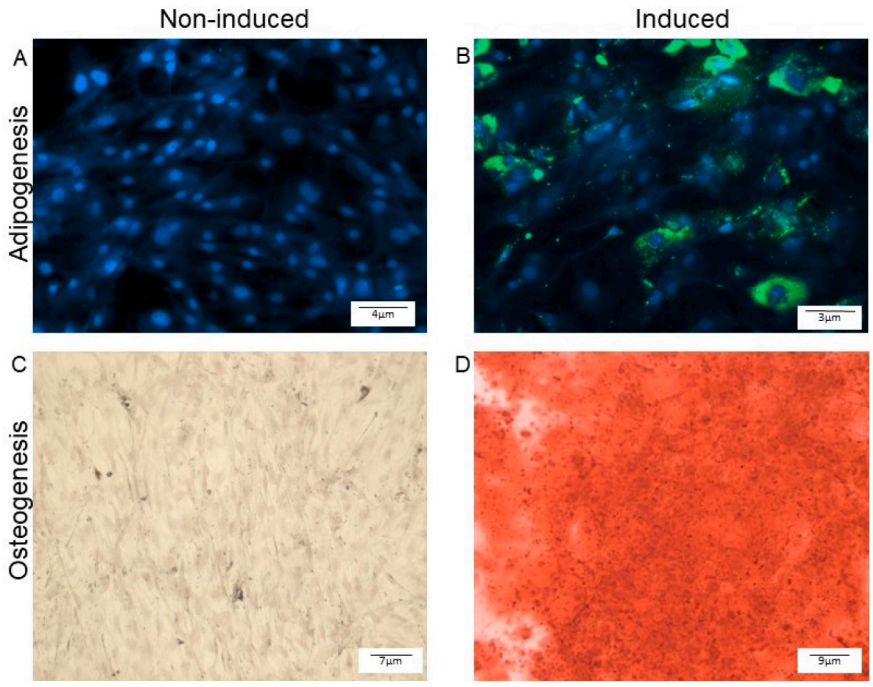

Fig 2. Adipogenic and osteogenic differentiation of mASCs: Representative microscopy images of mASCs induced to undergo adipogenic differentiation; (A) non-induced mASCs stained with DAPI and Nile red (no visible lipid droplet accumulation observed, indicating no differentiation). (B) Nile red-stained lipid droplets were observed in induced mASCs, confirming successful adipogenic differentiation. C – D; Osteogenic differentiation of mASCs; (C) non-induced mASCs stained with Alizarin red showed no calcium deposits present, (D) mASCs successfully differentiated into osteoblasts that contain calcium deposits that stain red. All images were taken at 10X magnification.

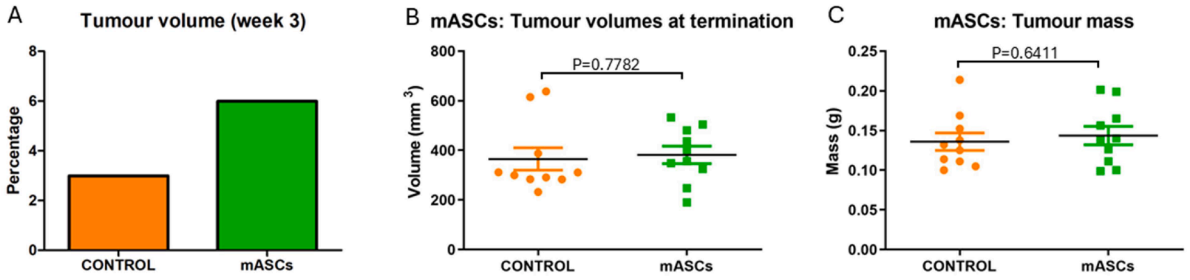

Fig 3. Tumour volume and mass. (A) A larger number of mice in the mASC group developed tumours earlier. On average, at termination, mammary tumour volume (B) and mass (C) were similar in both groups ($N = 10$ mice in each group).

3.4. mASC treatment enhances CD163+ M2 macrophage infiltration in mammary tumours but not in lung tissues

Immunohistochemical analysis was performed to evaluate the presence of CD163+ M2 macrophages in both lung and mammary FFPE tissue sections. Five randomly selected sections from each group (mASC-treated and untreated) were processed for immunohistochemistry. The percentage of positively stained cells was determined by dividing the total number of positive cells by the total number of all macrophages multiplied by 100. In mammary tumours, the mASC-treated group displayed a higher abundance of CD163+ M2-associated anti-inflammatory macrophages, as indicated by the presence of dark brown stained cells (Fig 5A). Quantitative analysis revealed a greater percentage of CD163+ macrophages in the mASC-treated group (Fig 5B). Conversely, in lung tissue, the mASC-treated group exhibited fewer CD163+ macrophages (Fig 5C). However, none of these results were statistically significant. The *p*-value for lung tissue was 0.0770 and in tumour tissue, it was 0.8763. Our findings suggest that mASC treatment contributes to a higher anti-inflammatory response in primary mammary tumours but not in lung tissues.

3.5. Increased infiltration of CD3+ T cells in mammary tumours and lung tissues following mASC treatment

Immunohistochemical analysis was conducted to evaluate the presence of CD3+ *T* cells in both lung and mammary tissue sections. Five randomly selected sections from both the mASC-treated and untreated groups were stained using a monoclonal antibody specific to the pan T-cell marker, CD3. In mammary tumours and lung tissues, an increased number of CD3+ *T* cells (stained dark brown) was observed in mASC-treated mice compared to the untreated group (Fig 6A). However, statistical analysis did not reveal a significant difference (mammary tumour $p = 0.3025$, lung tissue $p = 0.0938$) between the two groups (Figs 6B and 6C). These results reveal a trend towards an increase in CD3+ *T*-cell infiltration in mammary tumours and lung tissues of mASC-treated mice.

3.6. Differential gene expression profiles after mASC treatment in mammary and lung tissues

The effect of mASC treatment on gene expression in mammary and

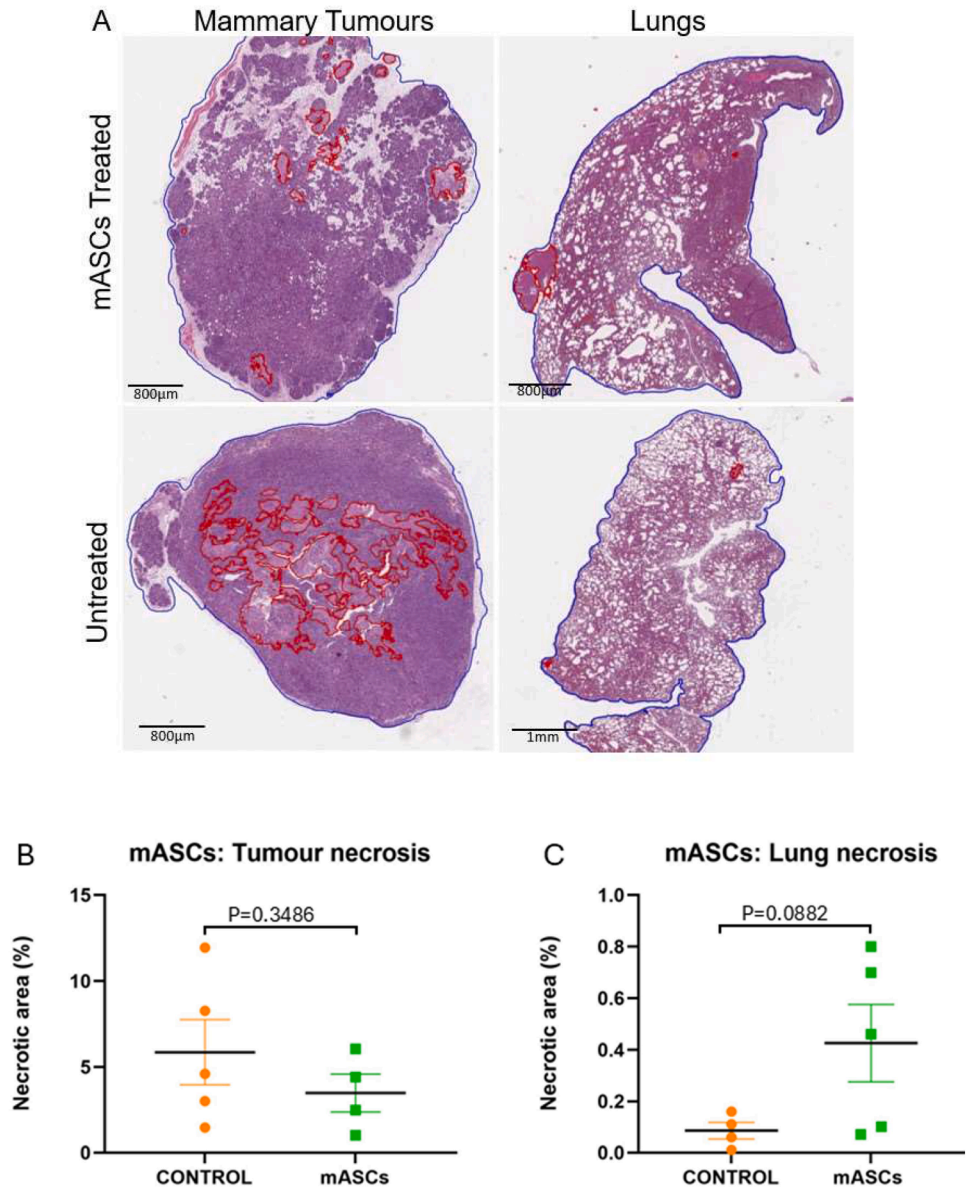

Fig 4. H&E sections of tumour and lung sections. Red boundaries encompassing necrotic tissues of mammary tumour and lung tissue. Scale bar represented by the horizontal line indicates lengths of 800 µm and 1 mm for mammary and lung tissues (A). (B) Tumour necrosis was lower in the mASC-treated group. (C) Higher levels of necrosis were observed in the lungs of the mASC-treated group ($N = 5$ in each group).

lung tissues was evaluated by analyzing the expression levels of five genes associated with BC growth and progression: *cd36, tgf-β3, vegfr1, eng* (cd105), and *mtdh*. The reference gene GAPDH (*gapdh*) was used as a control. In both primary mammary tumours and lungs of mASC-treated mice, the expression of *tgf-β3, vegfr1,* and *cd105* were all downregulated (Fig 7A-C). The expression of *mtdh* was similar to that of the control group in mammary tumours, while it was downregulated in the lungs (Fig 7D). Additionally, the expression of *cd36* was similar to controls in lung tissue but downregulated in mammary tumours (Fig 7E).

3.7. Increased plasma cytokine concentrations in response to mASC treatment

The plasma concentrations of all cytokines measured were higher in the mASC-treated group except for IL-27 ($p = 0.4463$) where no change was observed between untreated and treated groups. Although not statistically significant, the following cytokines were notably higher in the mASC-treated group when compared to controls (untreated): IFN-γ ($p = 0.3464$), IL-1α ($p = 0.5614$), IL-1β ($p = 0.2559$), IL-6 ($p = 0.2237$), IL-10 ($p = 0.2332$), IL-12p70 ($p = 0.5308$), IL-17A ($p = 0.2501$), and TNF-α ($p = 0.1399$). Additionally, MCP-1 ($p = 0.2405$), IL-23 ($p = 0.8053$), and IFN-β ($p = 0.3051$) also showed increased levels in the mASC-treated group (Fig 8).

4. Discussion

In this study, we investigated the influence of mASCs on breast cancer development and progression by using a mouse model of spontaneous mammary carcinogenesis. We believe this model more accurately reflects the expected outcomes should BC patients (humans) receive ASCs as cellular therapy. The isogeneic experimental design used in this study limits genetic variability, which has been a major limitation in previous studies and is therefore, we believe, likely to result in a more accurate reflection of the (human) clinical setting. Heterozygous female mice that spontaneously develop mammary tumours with lung metastasis were given either saline or mASC intraperitoneally over a 14-day

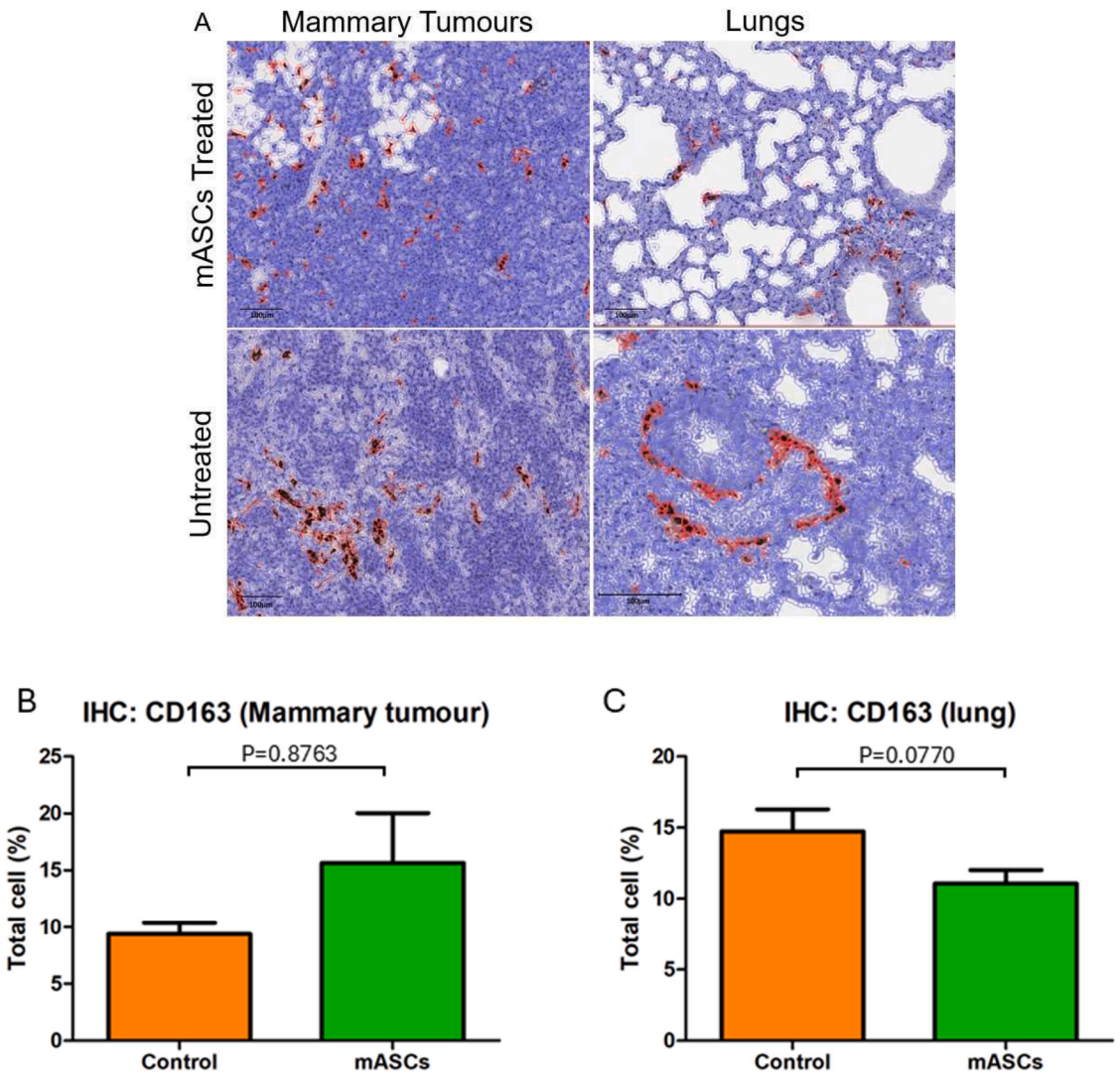

Fig 5. (A) Representative immunohistochemistry images of M2 macrophage involvement in primary mammary tumour and lung. CD163+ cells stained dark brown. Scale bar represented by the horizontal line indicates a length of 100 μm for all tissues. (B) and (C) Quantification of CD163+ macrophages in primary tumours and lungs, respectively. (B) Anti-inflammatory CD163+ macrophages were more frequent in the mASC-treated group. (C) Fewer CD163+ cells were observed in the mASC-treated group ($N = 5$ in each group).

period (3 different time points, 7 days apart) and were terminated 28 days after receiving the last dose. Although no significant differences in mammary tumour volume and mass were observed between the treated and untreated groups, it is noteworthy that twice as many mice in the mASC-treatment group developed palpable mammary tumours between days 60–65 from the time of birth compared to the control group. Lengyel et al. (2018) suggest that adipocytes and ASCs present in adipose tissue in close proximity to mammary glands secrete extracellular matrix molecules such as collagen IV and have been implicated in BC progression [57]. Furthermore, ASCs are known to secrete several growth factors, chemokines, and cytokines such as platelet-derived growth factor (PDGF-BB), chemokine ligand 5 (CCL5), VEGFA, VEGFB, stroma-derived factor 1α (SDF-1α), stem cell factor (SCF) and hepatocyte growth factor (HGF) that support BC cells proliferation in the TME [58]. Another study showed that WAT ASCs are recruited by tumours and promote growth [42]. BC xenograft studies have also reported an increase in proinflammatory cytokines that causes BC progression by stimulating growth in a paracrine manner [17,29,59]. We also observed a notable increase, although not significant, in proinflammatory cytokines (IFN-γ, IL-1α, IL-1β, IL-6, IL-17A, IL-12p70, and TNF-α) in the mASC treatment group. In this study, all 13 cytokines measured were higher in the mASC treatment group. Interleukin 10, which is also high, is a potent anti-inflammatory cytokine [60]. Eterno et al. (2014) using a xenograft model suggested that ASC-associated proinflammatory cytokines cause an increase in BC proliferation but do not maintain tumour growth [24]. ASCs are, therefore, not necessarily tumorigenic but rather exacerbate tumorigenic behaviour by creating an inflammatory environment [24]. The earlier detection of palpable tumours in the mASC-treatment group with no difference in tumour growth (volume and mass) observed in this study suggests that mASCs only exacerbate tumour initiation but not tumour progression.

Chemotherapeutic drugs eradicate cancer cells via necrosis [61]; therefore, the presence of necrotic tissue is an indicator of anti-tumour activity. In this study, more CD163+ macrophages and less necrotic tissue were observed in the mammary tumours of mASC-treated mice. However, lower numbers of M2-associated CD163+ macrophages and more necrotic tissue were observed in the lung of mASC-treated mice. The expression of CD163+ macrophages is used as a prognostic indicator for predicting BC recurrence-free survival [62]. An in vivo study found that high CD163 expression increased metastatic ability and tumorigenicity [62]. An increased number of CD163+ macrophages has been linked to reduced overall survival of BC patients, metastases, early

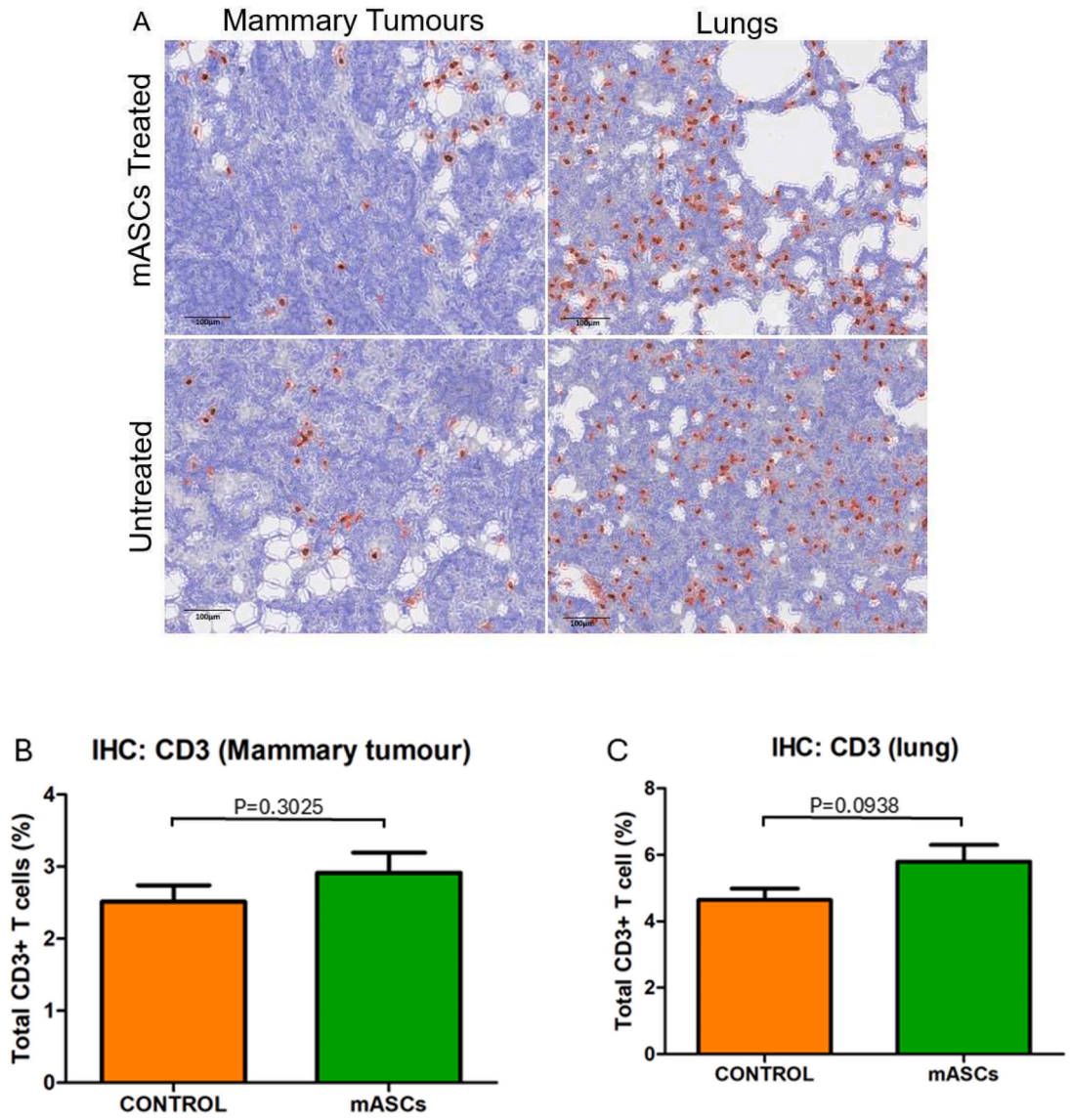

Fig 6. Representative immunohistochemistry images of CD3-positivity in primary mammary tumours and lung tissue. (A) CD3+ *T*-cells appear dark brown. The horizontal line on the image served as a scale bar, representing a uniform length of 100 μm. More CD3+ *T*-cells were observed in mammary tumours (B) and lung tissue (C) of mASC-treated mice ($N = 5$ mice in each group).

recurrence, and increased production of TGF-β1, IL-10 and VEGF [63,64]. Moreover, Shabo et al. (2008) demonstrated that CD163+ macrophages are present in greater numbers in the TME of advanced histological grade BC [62,64]. Therefore, an increase in the number of CD163+ macrophages is detrimental in BC, and this was only observed in mammary tumours and not in lungs of mASC-treated mice compared to controls. However, CD3+ *T*-cell numbers were greater in mASC-treated mice than in controls. High CD3 T numbers are associated with a decreased risk of relapse, favourable outcomes, and increased survival [65,66]. Thus, despite the higher number of CD163+ macrophages in mammary tumours, the high number of CD3+ *T*-cells in the mammary TME suggests the potential for an anti-tumour effect if the duration of treatment were extended.

In the primary mammary tumour, cd36 was downregulated but no change was observed in its expression in the lungs. cd36, a pro-tumour marker, is a transmembrane receptor involved in angiogenesis, apoptosis, adipocyte differentiation, immune signalling, and TGF-β activation [49,50,67]. Studies on a variety of human BC cell lines demonstrated that downregulation of cd36 expression supports the progression of an aggressive, metastatic and invasive tumour cell type, while upregulated cd36 was observed in non-aggressive BC cells [68,69]. The mouse FVB/N-Tg(MMTV-PyVT)634Mul/J model contains the PyVT oncogene that activates numerous pathways that lead to an aggressive tumour phenotype [70]. This may explain the downregulation of cd36 expression in mammary tumours and no change in expression in the lungs of mASC-treated mice. Therefore, the more aggressive the tumour, the lower the cd36 level, thus supporting tumour development and an increased the likelihood of having metastatic potential [67,69].

The expression of tgf-β3 and vegfr1 (FTL1) were downregulated in both primary mammary tumours and in the lungs in mASC-treated mice. In BC, these two genes are mainly involved in angiogenesis [71]. Downregulation of tgf-β3 has been associated with the early development of BC in ductal carcinoma in situ [72]. Furthermore, downregulated tgf-β3 is correlated with tgf-β3 gene loss of heterozygosity in human breast cancer [73]. Tgf-β3 restoration in mice inhibits tumour invasion, metastasis, and angiogenesis [73,74]. Moreover, tumour growth, metastasis, and angiogenesis were inhibited in a BC xenograft nude mouse model treated with tgf-β3 alone in vivo [74–76]. An in vivo study by Hank et al. (2020) demonstrated the lack of tgf-β3 expression

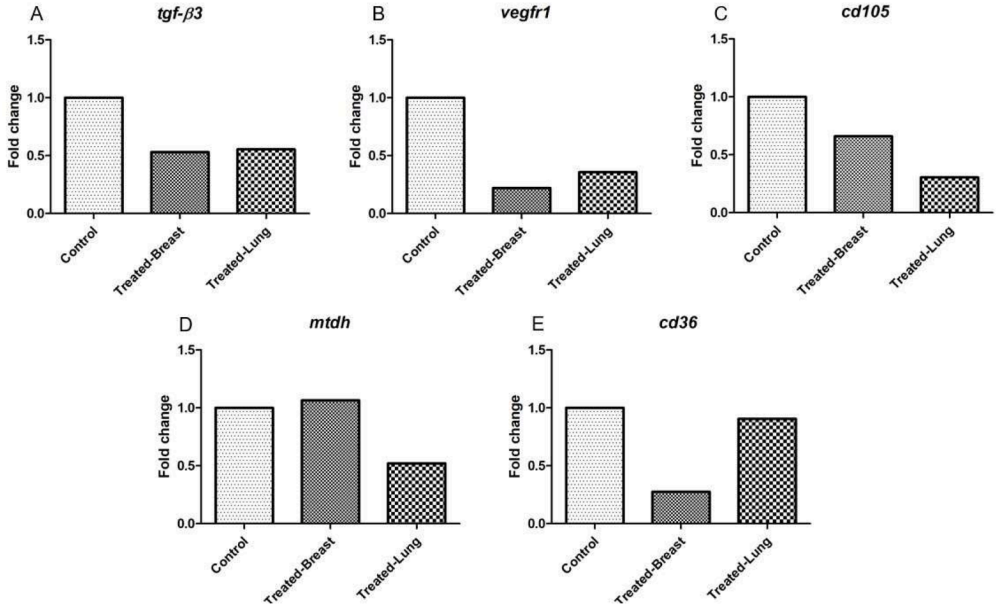

Fig 7. Fold change in gene expression within mammary and lung tissues of mice treated with mASCs, demonstrating SD<2 % ($N = 10$ in each group).

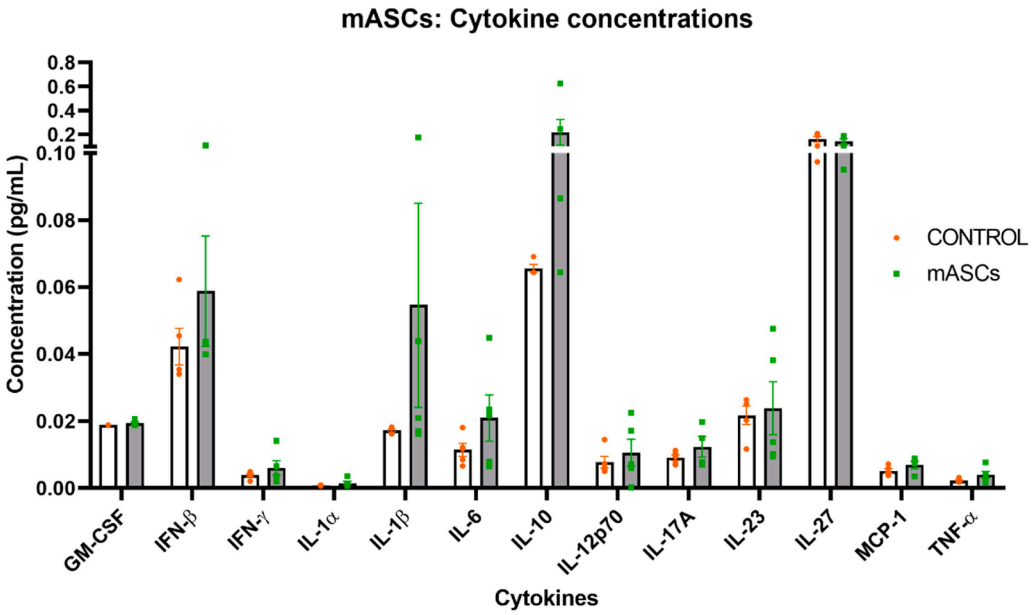

Fig 8. Plasma cytokine concentrations in control and mASC-treated groups: The concentration of all cytokines measured was higher in mice in the mASC group compared to those in the control group ($N = 5$ mice in each group). White bars represent cytokine levels observed in the control group. Grey bars represent cytokine levels observed in the mASC-treated group.

created an immunotolerant TME by increasing TGF-β signalling in the dendritic cell (DC) population and upregulated CCL22 myeloid DCs and indoleamine 2,3-dioxygenase (IDO) DCs [77]. Treg infiltration was mediated by these DCs, hence promoting BC development in the 4T1 murine BC model [77]. This study shows that mASC treatment downregulates tgf-β3, possibly creating a pro-tumour effect. Vascular endothelial growth factor interacts with vegfr1 to stimulate angiogenesis and is involved in BC development and metastasis [47]. Generally, vegfr1 is absent in healthy breast tissue but expressed in BC cells [78]. The expression of vegfr1 maintains the survival of BC cells and is associated with a poor prognosis in BC patients [78,79]. As long as vegfr1 is expressed, there is metastatic potential, but the degree of vegfr1 expression determines its tumorigenic and metastatic involvement. Various studies have reported that elevated expression of vegfr1 is linked to metastasis in multiple cancers including BC, and a shorter survival time [78,80–83]. The results of this study show that mASC-treatment exerts an anti-tumour effect by downregulating vegfr1 expression.

The expression of cd105 was also downregulated in both mammary tumours and in the lungs. Lack of or low expression of cd105 in primary mammary tumours is linked to gene methylation and poor clinical outcome in BC [84,85]. It has also been demonstrated that cd105 downregulation leads to increased invasion and tumorigenicity [86,87]. Additionally, cd105 overexpression decreases migration and metastasis [84,85]. Thus, mASC treatment may promote a pro-tumour effect by downregulating cd105 expression.

Mammary tumours did not show any change in the expression of mtdh, which was downregulated in pulmonary metastasis. Metadherin

is an oncogenic protein that promotes metastasis, cancer progression, and chemoresistance in mammary carcinoma [51,88]. Primary mammary tissues highly express mtdh compared to normal tissue [89]. Overexpression of mtdh correlates with an increased risk of relapse and poor disease-free survival [90]. This study therefore suggests that mASC treatment has an anti-tumour effect in pulmonary metastasis by downregulating mtdh expression.

The effect of mASC treatment on primary mammary and pulmonary metastatic tumours produced pleiotropic effects on the different molecular factors investigated. However, the combination of these varied molecular events resulted in a measurable phenotypic outcome which suggests a pro-tumour and anti-tumour effect of mASCs on mammary and pulmonary tumours, respectively. The pro-tumour effect exerted by mASC treatment includes the following; (i) double the number of mice in the mASC treatment group developed tumours early; (ii) more CD163+ macrophages were observed in mammary tumours of the mASC-treated mice; and (iii) downregulation of cd36, tgf-β3, and cd105, all of which are constituents that outweigh the anti-tumour effect exerted by the downregulation of vegfr1, thereby contributing to less necrosis observed in mammary tumours of mASC-treated mice. Although the number of CD3+ *T*-cells was higher in mASC-treated mice, this was not enough to render an anti-tumour effect. On the contrary, the anti-tumour effect produced by mASC treatment on pulmonary metastasis includes the following: (i) the lower number of CD163+ macrophages; (ii) the higher number of CD3+ *T*-cells; and (iii) the downregulation of mtdh and vegfr1, which is suggestive to be strong enough to outweigh the pro-tumour activity resulting from the downregulation of cd105 and tgf-β3, thereby increasing tumour necrosis. Furthermore, it is possible that the strong anti-tumour effect of mASCs observed in the lungs, but not in primary mammary tumours, may be the result of mASCs being trapped in the lungs [91]. This could suggest that there were fewer cells in the primary mammary tumour to render a net anti-tumour effect. It will be interesting to explore a different mode of administration, such as direct injection of mASCs into the mammary gland, to ensure that mASCs are present in that locale and then to investigate their effect on BC progression.

Our results highlight the differential effect of mASC treatment on different sites (mammary tumour and lung), underscoring the complexity of the therapeutic response in BC. The observed effect of mASC treatment on BC progression indicates its potential to modulate TME. The contrasting outcomes in different anatomical sites suggest that mASC interaction with other immunomodulators may lead to distinct outcomes in different anatomical TMEs, influencing tumour growth, necrosis, and potentially metastatic spread. These findings contribute to our understanding of the potential benefits and complexities associated with MSC-based therapies in BC. Further research in investigating the interaction of mASCs with other immune cells in the TME or the paracrine effect of mASCs on TME will further advance knowledge on the effect of mASC on BC progression at different anatomical sites.

While our study yields important findings, it is crucial to acknowledge several limitations. First, a larger sample size would have increased statistical power, allowing for a definitive conclusion. Second, extending beyond the time limits of this study. This could have provided a more comprehensive understanding of the impact of mASCs in the TME and allowed for the assessment of metastatic potential beyond the lungs. Future studies should consider extending the observation period and exploring additional metastatic sites. There is a need for greater insight into the underlying mechanisms involved in order to understand the site-specific interactions between mASCs and the TME.

5. Conclusions

In an attempt to recapitulate the clinical scenario of individuals with BC receiving MSC treatment and to investigate the possible outcomes of such treatment, an isogenic experimental design was used to investigate the effect of mASCs on BC progression in a transgenic MMTV-PyMT mouse model that spontaneously develops a mammary tumour with pulmonary metastasis. This study suggests that mASC treatment produced a pleiotropic effect on BC progression by demonstrating pro-tumour activity on primary mammary tumours and anti-tumour activity on pulmonary metastatic tumours, resulting in less and more tumour necrosis respectively at these sites.

Data availability

The data that support the findings of this study are available upon reasonable request from the corresponding author.

Institutional review board statement

The animal study protocol was approved by the Faculty of Health Sciences Research Ethics Committee (ethics reference no.: REC166–19) and the Animal Ethics Committee (ethics reference no.: 534/2019) of the University of Pretoria.

CRediT authorship contribution statement

Kimberly T. Peta: Writing – review & editing, Writing – original draft, Visualization, Project administration, Methodology, Investigation, Formal analysis, Data curation. **Chrisna Durandt:** Writing – review & editing, Visualization, Validation, Supervision, Project administration, Methodology, Formal analysis, Data curation. **Marlene B. van Heerden:** Writing – review & editing, Visualization, Validation, Project administration, Methodology, Investigation, Data curation. **Michael S. Pepper:** Writing – review & editing, Visualization, Validation, Supervision, Resources, Project administration, Methodology, Investigation, Funding acquisition, Conceptualization. **Melvin A. Ambele:** Writing – review & editing, Visualization, Validation, Supervision, Resources, Project administration, Methodology, Investigation, Funding acquisition, Formal analysis, Data curation, Conceptualization.

Declaration of competing interest

The authors declare that they have no known competing financial interests or personal relationships that could have appeared to influence the work reported in this paper.

Funding

M.A.A is supported by the South African Medical Research Council Self-Initiated Research Grant (grant no. A1A982); and by the National Research Foundation Competitive Support for Unrated Researchers (grant no. 114044); M.S.P is supported by grants from the South African Medical Research Council University Flagship Project (SAMRC-RFA-UFSP-01-2013/STEM CELLS), the SAMRC Extramural Unit for Stem Cell Research and Therapy, and the Institute for Cellular and Molecular Medicine of the University of Pretoria.

Acknowledgements

We extend our sincere gratitude to the dedicated team at OVARU for their exceptional care of the mice used in this study. Special appreciation is extended to Mrs. Ilse Janse van Rensburg, Mr. Muchavengwa Chovheya, Dr. Richard Mavunganidze, and Mr. Humbelani Ratshivhanda. Furthermore, we express our deep appreciation to Prof. Piet Becker for his assistance with statistics.

References

[1] Bray F, Ferlay J, Soerjomataram I, Siegel RL, Torre LA, Jemal A. Global cancer statistics 2018: GLOBOCAN estimates of incidence and mortality worldwide for 36 cancers in 185 countries. CA Cancer J Clin 2018;68:394–424. https://doi.org/10.3322/caac.21492.

[2] Sung H, Ferlay J, Siegel RL, Laversanne M, Soerjomataram I, Jemal A, et al. Global cancer statistics 2020: GLOBOCAN estimates of incidence and mortality worldwide for 36 cancers in 185 countries. CA Cancer J Clin 2021;71:209–49.

[3] DeSantis CE, Lin CC, Mariotto AB, Siegel RL, Stein KD, Kramer JL, et al. Cancer treatment and survivorship statistics, 2014. CA Cancer J Clin 2014;64:252–71. https://doi.org/10.3322/caac.21235.

[4] Zhou J, Zhong Y. Breast cancer immunotherapy. Cell Mol Immunol 2004;1:247–55.

[5] Reagan MR, Kaplan DL. Concise review: mesenchymal stem cell tumor-homing: detection methods in disease model systems. Stem cells 2011;29:920–7.

[6] El-Haibi CP, Karnoub AE. Mesenchymal stem cells in the pathogenesis and therapy of breast cancer. J Mammary Gland Biol Neoplasia 2010;15:399–409.

[7] Almeida-Porada G, Atala AJ, Porada CD. Therapeutic Mesenchymal Stromal Cells for Immunotherapy and for Gene and Drug Delivery. Mol Ther Methods Clin Dev 2020;16:204–24. https://doi.org/10.1016/j.omtm.2020.01.005.

[8] Fajka-Boja R, Szebeni GJ, Hunyadi-Gulyás É, Puskás LG, Katona RL. Polyploid Adipose Stem Cells Shift the Balance of IGF1/IGFBP2 to Promote the Growth of Breast Cancer. Front Oncol 2020;10:1–8. https://doi.org/10.3389/fonc.2020.00157.

[9] Karnoub AE, Dash AB, Vo AP, Sullivan A, Brooks MW, Bell GW, et al. Mesenchymal stem cells within tumour stroma promote breast cancer metastasis. Nature 2007;449:557–63.

[10] Alonso-Goulart V, Ferreira LB, Duarte CA, Lima IL, Ferreira ER, Oliveira BC, et al. Mesenchymal stem cells from human adipose tissue and bone repair: a literature review. Biotechnol Res Innov 2018;2:74–80. https://doi.org/10.1016/j.biori.2017.10.005.

[11] Kothari C, Diorio C, Durocher F. The Importance of Breast Adipose Tissue in Breast Cancer. Int J Mol Sci 2020;21:1–34.

[12] Yan X, Fu C, Chen L, Qin J, Zeng Q, Yuan H, et al. Mesenchymal stem cells from primary breast cancer tissue promote cancer proliferation and enhance mammosphere formation partially via EGF/EGFR/Akt pathway. Breast Cancer Res Treat 2012;132:153–64.

[13] Goldstein RH, Reagan MR, Anderson K, Kaplan DL, Rosenblatt M. Human bone marrow–derived MSCs can home to orthotopic breast cancer tumors and promote bone metastasis. Cancer Res 2010;70:10044–50.

[14] Albarenque SM, Zwacka RM, Mohr A. Both human and mouse mesenchymal stem cells promote breast cancer metastasis. Stem Cell Res 2011;7:163–71.

[15] Yu P, Huang Y, Han Y, Lin L, Sun W, Rabson A, et al. TNFα-activated mesenchymal stromal cells promote breast cancer metastasis by recruiting CXCR2+ neutrophils. Oncogene 2017;36:482–90.

[16] Zimmerlin L, Donnenberg AD, Rubin JP. Regenerative Therapy and Cancer: in Vitro and In Vivo Studies of the Interaction Between Adipose-Derived Stem Cells and Breast Cancer Cells from Clinical Isolates. Tissue Eng 2010;17:1–14.

[17] Walter M, Liang S, Ghosh S, Hornsby P, Li R. Interleukin 6 secreted from adipose stromal cells promotes migration and invasion of breast cancer cells. Oncogene 2009;28:2745–55.

[18] Sakurai M, Miki Y, Takagi K, Suzuki T, Ishida T, Ohuchi N, et al. Interaction with adipocyte stromal cells induces breast cancer malignancy via S100A7 upregulation in breast cancer microenvironment. Breast Cancer Res 2017;19:1–12. https://doi.org/10.1186/s13058-017-0863-0.

[19] Zhao Y, Zhang X, Zhao H, Wang J, Zhang Q. CXCL5 secreted from adipose tissue-derived stem cells promotes cancer cell proliferation. Oncol Lett 2018;15:1403–10.

[20] Hillers LE, D'Amato JV, Chamberlin T, Paderta G, Arendt LM. Obesity-Activated Adipose-Derived Stromal Cells Promote Breast Cancer Growth and Invasion. Neoplasia 2018;20:1161–74. https://doi.org/10.1016/j.neo.2018.09.004.

[21] Su F, Wang X, Pearson T, Lee J, Krishnamurthy S, Ueno NT, et al. Ablation of Stromal Cells with a Targeted Proapoptotic Peptide Suppresses Cancer Chemotherapy Resistance and Metastasis. Mol Ther - Oncolytics 2020;18:579–86. https://doi.org/10.1016/j.omto.2020.08.012.

[22] Rowan BG, Gimble JM, Sheng M, Anbalagan M, Jones RK, Frazier TP, et al. Human Adipose Tissue-Derived Stromal/Stem Cells Promote Migration and Early Metastasis of Triple Negative Breast Cancer Xenografts. PLOS ONE 2014;9:1–13. https://doi.org/10.1371/journal.pone.0089595.

[23] Orecchioni S, Gregato G, Martin-Padura I, Reggiani F, Braidotti P, Mancuso P, et al. Complementary populations of human adipose CD34+ progenitor cells promote growth, angiogenesis, and metastasis of breast cancer. Cancer Res 2013;73:5880–91.

[24] Eterno V, Zambelli A, Pavesi L, Villani L, Zanini V, Petrolo G, et al. Mesenchymal Stem Cells (ASCs) may favour breast cancer recurrence via HGF/c-Met signaling. Oncotarget 2014;5:613–33. https://doi.org/10.18632/oncotarget.1359.

[25] Ritter A, Friemel A, Fornoff F, Adjan M, Solbach C, Yuan J, et al. Characterization of adipose-derived stem cells from subcutaneous and visceral adipose tissues and their function in breast cancer cells. Oncotarget 2015;6:34475–93. https://doi.org/10.18632/oncotarget.5922.

[26] Tsuji W, Rubin JP, Marra KG. Adipose-derived stem cells: implications in tissue regeneration. World J Stem Cells 2014;6:312–21. https://doi.org/10.4252/wjsc.v6.i3.312.

[27] Zhao R, Kaakati R, Liu X, Xu L, Lee AK, Bachelder R, et al. CRISPR/Cas9-Mediated BRCA1 Knockdown Adipose Stem Cells Promote Breast Cancer Progression. Plast Reconstr Surg 2019;143:747–56. https://doi.org/10.1097/PRS.0000000000005316.

[28] Charvet HJ, Orbay H, Harrison L, Devi K, Sahar DE. In vitro effects of adipose-derived stem cells on breast cancer cells harvested from the same patient. Ann Plast Surg 2016;76:S241–5.

[29] Sabol RA, Bowles AC, Côté A, Wise R, O'Donnell B, Matossian MD, et al. Leptin produced by obesity-altered adipose stem cells promotes metastasis but not tumorigenesis of triple-negative breast cancer in orthotopic xenograft and patient-derived xenograft models. Breast Cancer Res 2019;21:1–14. https://doi.org/10.1186/s13058-019-1153-9.

[30] Mishra AK, Parish CR, Wong ML, Licinio J, Blackburn AC. Leptin signals via TGFB1 to promote metastatic potential and stemness in breast cancer. PLOS ONE 2017;12:1–21. https://doi.org/10.1371/journal.pone.0178454.

[31] Scioli MG, Artuso S, D'Angelo C, Porru M, D'Amico F, Bielli A, Orlandi A. Adipose-derived stem cell-mediated paclitaxel delivery inhibits breast cancer growth. PLOS ONE 2018;13:1–16. https://doi.org/10.1371/journal.pone.0203426.

[32] Martin FT, Dwyer RM, Kelly J, Khan S, Murphy JM, et al. Potential role of mesenchymal stem cells (MSCs) in the breast tumour microenvironment: stimulation of epithelial to mesenchymal transition (EMT). Breast Cancer Res Treat 2010;124:317–26. https://doi.org/10.1007/s10549-010-0734-1.

[33] Kalimuthu S, Gangadaran P, Rajendran RL, Zhu L, Oh JM, Lee HW, et al. A New Approach for Loading Anticancer Drugs Into Mesenchymal Stem Cell-Derived Exosome Mimetics for Cancer Therapy. Front Pharmacol 2018;9:1–10. https://doi.org/10.3389/fphar.2018.01116.

[34] Li T, Zhou X, Wang J, Liu Z, Han S, Wan L, et al. Adipose-derived mesenchymal stem cells and extracellular vesicles confer antitumor activity in preclinical treatment of breast cancer. Pharmacol Res 2020;157:1–9. https://doi.org/10.1016/j.phrs.2020.104843.

[35] Moraes DA, Sibov TT, Pavon LF, Alvim PQ, Bonadio RS, Da Silva JR, et al. A reduction in CD90 (THY-1) expression results in increased differentiation of mesenchymal stromal cells. Stem Cell Res Ther 2016;7:1–14. https://doi.org/10.1186/s13287-016-0359-3.

[36] Ryu H, Oh JE, Rhee KJ, Baik SK, Kim J, Kang SJ, et al. Adipose tissue-derived mesenchymal stem cells cultured at high density express IFN-β and suppress the growth of MCF-7 human breast cancer cells. Cancer Lett 2014;352:220–7.

[37] Ejaz A, Yang KS, Venkatesh P, Chinnapaka S, Kokai LE, Rubin JP. The Impact of Human Lipoaspirate and Adipose Tissue-Derived Stem Cells Contact Culture on Breast Cancer Cells: implications in Breast Reconstruction. Int J Mol Sci 2020;21:1–18.

[38] Sun B, Roh KH, Park JR, Lee SR, Park SB, Jung JW, et al. Therapeutic potential of mesenchymal stromal cells in a mouse breast cancer metastasis model. Cytotherapy 2009;11:289–98.

[39] Clarke MR, Imhoff FM, Baird SK. Mesenchymal stem cells inhibit breast cancer cell migration and invasion through secretion of tissue inhibitor of metalloproteinase-1 and-2. Mol Carcinog 2015;54:1214–9.

[40] Shojaei S, Hashemi SM, Ghanbarian H, Sharifi K, Salehi M, Mohammadi-Yeganeh S. Delivery of miR-381-3p Mimic by Mesenchymal Stem Cell-Derived Exosomes Inhibits Triple Negative Breast Cancer Aggressiveness; an In Vitro Study. Stem Cell Rev Rep 2021;17:1027–38. https://doi.org/10.1007/s12015-020-10089-4.

[41] Oloyo AK, Ambele MA, Pepper MS. Contrasting views on the role of mesenchymal stromal/stem cells in tumour growth: a systematic review of experimental design. Stem Cells 2017:103–24.

[42] Zhang Y, Daquinag A, Traktuev DO, Amaya-Manzanares F, Simmons PJ, March KL, et al. White Adipose Tissue Cells Are Recruited by Experimental Tumors and Promote Cancer Progression in Mouse Models. Cancer Res 2009;69:5259–66. https://doi.org/10.1158/0008-5472.Can-08-3444.

[43] Li W, Xu H, Qian C. c-Kit-Positive Adipose Tissue-Derived Mesenchymal Stem Cells Promote the Growth and Angiogenesis of Breast Cancer. Biomed Res Int 2017;2017:1–12. https://doi.org/10.1155/2017/7407168.

[44] Xu H, Li W, Luo S, Yuan J, Hao L. Adipose derived stem cells promote tumor metastasis in breast Cancer cells by stem cell factor inhibition of miR20b. Cell Signal 2019;62:1–10. https://doi.org/10.1016/j.cellsig.2019.109350.

[45] Attalla S, Taifour T, Bui T, Muller W. Insights from transgenic mouse models of PyMT-induced breast cancer: recapitulating human breast cancer progression in vivo. Oncogene 2021;40:475–91. https://doi.org/10.1038/s41388-020-01560-0.

[46] Esquivel-Velázquez M, Ostoa-Saloma P, Palacios-Arreola MI, Nava-Castro KE, Castro JI, Morales-Montor J. The role of cytokines in breast cancer development and progression. J Interferon Cytokine Res 2015;35:1–16.

[47] Castañeda-Gill JM, Vishwanatha JK. Antiangiogenic mechanisms and factors in breast cancer treatment. J Carcinog 2016;15:1–10. https://doi.org/10.4103/1477-3163.176223.

[48] Bernabeu C, Lopez-Novoa JM, Quintanilla M. The emerging role of TGF-β superfamily coreceptors in cancer. Biochim Biophys Acta (BBA) - Mol Basis Dis 2009;1792:954–73. https://doi.org/10.1016/j.bbadis.2009.07.003.

[49] DeFilippis RA, Chang H, Dumont N, Rabban JT, Chen YY, Fontenay GV, et al. CD36 Repression Activates a Multicellular Stromal Program Shared by High Mammographic Density and Tumor TissuesCD36 Modulates Phenotypes of Breast Density and Desmoplasia. Cancer Discov 2012;2:826–39.

[50] Hale JS, Li M, Sinyuk M, Jahnen-Dechent W, Lathia JD, Silverstein RL. Context dependent role of the CD36-thrombospondin-histidine-rich glycoprotein axis in tumor angiogenesis and growth. PloS one 2012;7:1–11.

[51] Yin Q, Han Y, Zhu D, Li Z, Shan S, Jin W, et al. miR-145 and miR-497 suppress TGF-β-induced epithelial–mesenchymal transition of non-small cell lung cancer by targeting MTDH. Cancer Cell Int 2018;18:1–9. https://doi.org/10.1186/s12935-018-0601-4.

[52] Ambele MA, Dessels C, Durandt C, Pepper MS. Genome-wide analysis of gene expression during adipogenesis in human adipose-derived stromal cells reveals novel patterns of gene expression during adipocyte differentiation. Stem Cell Res 2016;16:725–34. https://doi.org/10.1016/j.scr.2016.04.011.

[53] Seavey JG, Wheatley BM, Pavey GJ, Tomasino AM, Hanson MA, Sanders EM, et al. Early local delivery of vancomycin suppresses ectopic bone formation in a rat

model of trauma-induced heterotopic ossification. J Orthopaed Res 2017;35:2397–406. https://doi.org/10.1002/jor.23544.
[54] Koch TG, Heerkens T, Thomsen PD, Betts DH. Isolation of mesenchymal stem cells from equine umbilical cord blood. BMC Biotechnol 2007;7:26. https://doi.org/10.1186/1472-6750-7-26.
[55] Dhanraj P, van Heerden MB, Pepper MS, Ambele MA. Sexual Dimorphism in Changes That Occur in Tissues, Organs and Plasma during the Early Stages of Obesity Development. Biol (Basel) 2021;10:1–22.
[56] Pitere RR, van Heerden MB, Pepper MS, Ambele MA. Slc7a8 Deletion Is Protective against Diet-Induced Obesity and Attenuates Lipid Accumulation in Multiple Organs. Biol (Basel) 2022;11:374–84.
[57] Lengyel E, Makowski L, DiGiovanni J, Kolonin MG. Cancer as a Matter of Fat: the Crosstalk between Adipose Tissue and Tumors. Trends Cancer 2018;4:374–84. https://doi.org/10.1016/j.trecan.2018.03.004.
[58] Kucerova L, Kovacovicova M, Polak S, Bohac M, Fedeles J, Palencar D. Interaction of human adipose tissue-derived mesenchymal stromal cells with breast cancer cells. Neoplasma 2011;58:1–10.
[59] Bandini E, Rossi T, Gallerani G, Fabbri F. Adipocytes and microRNAs Crosstalk: a Key Tile in the Mosaic of Breast Cancer Microenvironment. Cancers (Basel) 2019;11:1–13.
[60] Hamidullah Changkija B, Konwar R. Role of interleukin-10 in breast cancer. Breast Cancer Res Treat 2012;133:11–21. https://doi.org/10.1007/s10549-011-1855-x.
[61] Zhang J, Lou X, Jin L, Zhou R, Liu S, Xu N, et al. Necrosis, and then stress induced necrosis-like cell death, but not apoptosis, should be the preferred cell death mode for chemotherapy: clearance of a few misconceptions. Oncoscience 2014;1:407–22. https://doi.org/10.18632/oncoscience.61.
[62] Ding J, Jin W, Chen C, Shao Z, Wu J. Tumor Associated Macrophage × Cancer Cell Hybrids May Acquire Cancer Stem Cell Properties in Breast Cancer. PLOS ONE 2012;7:1–12. https://doi.org/10.1371/journal.pone.0041942.
[63] Larionova I, Kazakova E, Patysheva M, Kzhyshkowska J. Transcriptional, epigenetic and metabolic programming of tumor-associated macrophages. Cancers (Basel) 2020;12:1–41.
[64] Shabo I, Stål O, Olsson H, Doré S, Svanvik J. Breast cancer expression of CD163, a macrophage scavenger receptor, is related to early distant recurrence and reduced patient survival. Int J Cancer 2008;123:780–6. https://doi.org/10.1002/ijc.23527.
[65] Tsiatas M, Kalogeras KT, Manousou K, Wirtz RM, Gogas H, Veltrup E, et al. Evaluation of the prognostic value of CD3, CD8, and FOXP3 mRNA expression in early-stage breast cancer patients treated with anthracycline-based adjuvant chemotherapy. Cancer Med 2018;7:5066–82.
[66] Gomez-Macias GS, Molinar-Flores G, Lopez-Garcia CA, Santuario-Facio S, Decanini-Arcaute H, Valero-Elizondo J, et al. Immunotyping of tumor-infiltrating lymphocytes in triple-negative breast cancer and genetic characterization. Oncol Lett 2020;20:1–10.
[67] Wang J, Li Y. CD36 tango in cancer: signaling pathways and functions. Theranostics 2019;9:4893–908. https://doi.org/10.7150/thno.36037.
[68] Gyamfi J, Yeo JH, Kwon D, Min BS, Cha YJ, Koo JS, et al. Interaction between CD36 and FABP4 modulates adipocyte-induced fatty acid import and metabolism in breast cancer. npj Breast Cancer 2021;7:1–18. https://doi.org/10.1038/s41523-021-00324-7.
[69] Uray IP, Liang Y, Hyder SM. Estradiol down-regulates CD36 expression in human breast cancer cells. Cancer Lett 2004;207:101–7. https://doi.org/10.1016/j.canlet.2003.10.021.
[70] Shishido S, Delahaye A, Beck A, Nguyen T. The MMTV-PyVT Transgenic Mouse as a Multistage Model for Mammary Carcinoma and the Efficacy of Antineoplastic Treatment. J Cancer Ther 2013;04:1187–97. https://doi.org/10.4236/jct.2013.47138.
[71] Oklu R, Walker TG, Wicky S, Hesketh R. Angiogenesis and Current Antiangiogenic Strategies for the Treatment of Cancer. J Vasc Interv Radiol 2010;21:1791–805. https://doi.org/10.1016/j.jvir.2010.08.009.
[72] Gatza CE, Oh SY, Blobe GC. Roles for the type III TGF-β receptor in human cancer. Cell Signal 2010;22:1163–74. https://doi.org/10.1016/j.cellsig.2010.01.016.
[73] Sun L, Chen C. Expression of transforming growth factor β type III receptor suppresses tumorigenicity of human breast cancer MDA-MB-231 cells. J Biol Chem 1997;272:25367–72.
[74] Dong M, How T, Kirkbride KC, Gordon KJ, Lee JD, Hempel N, et al. The type III TGF-β receptor suppresses breast cancer progression. J Clin Invest 2007;117:206–17.
[75] Bandyopadhya A, Zhu Y, Cibull ML, Bao L, Chen C, Sun L. A soluble transforming growth factor β type III receptor suppresses tumorigenicity and metastasis of human breast cancer MDA-MB-231 cells. Cancer Res 1999;59:5041–6.
[76] Bandyopadhyay A, Zhu Y, Malik SN, Kreisberg J, Brattain MG, Sprague EA, et al. Extracellular domain of TGFβ type III receptor inhibits angiogenesis and tumor growth in human cancer cells. Oncogene 2002;21:3541–51.
[77] Hanks BA, Holtzhausen A, Evans KS, Jamieson R, Gimpel P, Campbell OM, et al. Type III TGF-β receptor downregulation generates an immunotolerant tumor microenvironment. J Clin Invest 2020;123:3925–40.
[78] Ning Q, Liu C, Hou L, Meng M, Zhang X, Luo M, et al. Vascular Endothelial Growth Factor Receptor-1 Activation Promotes Migration and Invasion of Breast Cancer Cells through Epithelial-Mesenchymal Transition. PLOS ONE 2013;8:1–11. https://doi.org/10.1371/journal.pone.0065217.
[79] Lee TH, Seng S, Sekine M, Hinton C, Fu Y, Avraham HK, et al. Vascular Endothelial Growth Factor Mediates Intracrine Survival in Human Breast Carcinoma Cells through Internally Expressed VEGFR1/FLT1. PLoS Med 2007;4:1–16. https://doi.org/10.1371/journal.pmed.0040186.
[80] Mimori K, Fukagawa T, Kosaka Y, Kita Y, Ishikawa K, Etoh T, et al. Hematogenous Metastasis in Gastric Cancer Requires Isolated Tumor Cells and Expression of Vascular Endothelial Growth Factor Receptor-1. Clin Cancer Res 2008;14:2609–16. https://doi.org/10.1158/1078-0432.Ccr-07-4354.
[81] Kourea HP, Dimitrakopoulos FI, Koliou GA, Batistatou A, Papadopoulou K, Bobos M, et al. Clinical Significance of Major Angiogenesis-Related Effectors in Patients with Metastatic Breast Cancer Treated with Trastuzumab-Based Regimens. J Korean Cancer Assoc 2021;0:1053–64. https://doi.org/10.4143/crt.2021.748.
[82] Laird A, O'Mahony FC, Nanda J, Riddick ACP, O'Donnell M, Harrison DJ, et al. Differential Expression of Prognostic Proteomic Markers in Primary Tumour, Venous Tumour Thrombus and Metastatic Renal Cell Cancer Tissue and Correlation with Patient Outcome. PLOS ONE 2013;8:1–14. https://doi.org/10.1371/journal.pone.0060483.
[83] Goussia A, Simou N, Zagouri F, Manousou K, Lazaridis G, Gogas H, et al. Associations of angiogenesis-related proteins with specific prognostic factors, breast cancer subtypes and survival outcome in early-stage breast cancer patients. A Hellenic Cooperative Oncology Group (HeCOG) trial. PLOS ONE 2018;13:1–19. https://doi.org/10.1371/journal.pone.0200302.
[84] González Muñoz T, Amaral AT, Puerto-Camacho P, Peinado H, de Álava E. Endoglin in the Spotlight to Treat Cancer. Int J Mol Sci 2021;22:1–24. https://doi.org/10.3390/ijms22063186.
[85] Pérez-Gómez E, del Castillo G, Santibáñez JF, Lêpez-Novoa JM, Bernabéu C, Quintanilla M. The Role of the TGF-β Coreceptor Endoglin in Cancer. ScientificWorldJournal 2010;10:1–19. https://doi.org/10.1100/tsw.2010.230.
[86] Henry LA, Johnson DA, Sarrió D, Lee S, Quinlan PR, Crook T, et al. Endoglin expression in breast tumor cells suppresses invasion and metastasis and correlates with improved clinical outcome. Oncogene 2011;30:1046–58. https://doi.org/10.1038/onc.2010.488.
[87] Subramaniam V, Chakrabarti R, Prud'homme GJ, Jothy S. Tranilast inhibits cell proliferation and migration and promotes apoptosis in murine breast cancer. Anticancer Drugs 2010;21:351–61. https://doi.org/10.1097/CAD.0b013e328334992c.
[88] Gollavilli PN, Kanugula AK, Koyyada R, Karnewar S, Neeli PK, Kotamraju S. AMPK inhibits MTDH expression via GSK3β and SIRT1 activation: potential role in triple negative breast cancer cell proliferation. FEBS J 2015;282:3971–85. https://doi.org/10.1111/febs.13391.
[89] Nguyen YTK, Moon JY, Ediriweera MK, Cho SK. Phenethyl Isothiocyanate Suppresses Stemness in the Chemo- and Radio-Resistant Triple-Negative Breast Cancer Cell Line MDA-MB-231/IR Via Downregulation of Metadherin. Cancers (Basel) 2020;12:1–18.
[90] Ward A, Balwierz A, Zhang JD, Küblbeck M, Pawitan Y, Hielscher T, et al. *Re*-expression of microRNA-375 reverses both tamoxifen resistance and accompanying EMT-like properties in breast cancer. Oncogene 2013;32:1173–82. https://doi.org/10.1038/onc.2012.128.
[91] Kallmeyer K, André-Lévigne D, Baquié M, Krause KH, Pepper MS, et al. Fate of systemically and locally administered adipose-derived mesenchymal stromal cells and their effect on wound healing. Stem Cells Transl Med 2020;9:131–44. https://doi.org/10.1002/sctm.19-0091.